HHS Public Access

Author manuscript

J Biomech. Author manuscript; available in PMC 2017 December 08.

Published in final edited form as:

J Biomech. 2016 December 08; 49(16): 4173–4179. doi:10.1016/j.jbiomech.2016.11.051.

Novel multi-functional fluid flow device for studying cellular mechanotransduction

James S. Lyons[a], **Shama R. Iyer**[a], **Richard M. Lovering**[a], **Christopher W. Ward**[b], and **Joseph P. Stains**[a,*]

[a]Department of Orthopaedics, University of Maryland School of Medicine, Baltimore MD, 21201, USA

[b]University of Maryland School of Nursing, Baltimore MD, 21201, USA

Abstract

Cells respond to their mechanical environment by initiating multiple mechanotransduction signaling pathways. Defects in mechanotransduction have been implicated in a number of pathologies; thus, there is need for convenient and efficient methods for studying the mechanisms underlying these processes. A widely used and accepted technique for mechanically stimulating cells in culture is the introduction of fluid flow on cell monolayers. Here, we describe a novel, multifunctional fluid flow device for exposing cells to fluid flow in culture. This device integrates with common lab equipment including routine cell culture plates and peristaltic pumps. Further, it allows the fluid flow treated cells to be examined with outcomes at the cell and molecular level. We validated the device using the biologic response of cultured UMR-106 osteoblast-like cells in comparison to a commercially available system of laminar sheer stress to track live cell calcium influx in response to fluid flow. In addition, we demonstrate the fluid flow-dependent activation of phospho-ERK in these cells, consistent with the findings in other fluid flow devices. This device provides a low cost, multi-functional alternative to currently available systems, while still providing the ability to generate physiologically relevant conditions for studying processes involved in mechanotransduction *in vitro*.

Keywords

fluid shear stress; osteoblast; osteocyte; bone cells; signal transduction; mechanotransduction; intracellular calcium

* Corresponding Author: 100 Penn Street, Allied Heath Building, Room 540E, Baltimore, MD 21201, Phone: (410) 706-2494, jstains@som.umaryland.edu.

Conflict of Interest Statement

The authors (JSL, CWW, JPS) are listed as inventors on pending patent application related to technology described in this work (US Provisional Patent Number: 62/311,654 filed on March 22, 2016).

1. Introduction

Cells respond to their mechanical environment by activating biochemical signaling pathways, a process known as mechanotransduction. Mechanotransduction regulates diverse physiologic function in healthy cells and burgeoning evidence implicates dysregulation of mechanotransduction cascades in disease pathology (Jaalouk and Lammerding, 2009). Given that these mechanotransduction pathways often integrate multiple signaling events, there is a growing interest to identify key signaling nodes that can be targeted to modulate outputs that drive physiology or disease.

In the skeletal system, osteocytes sense mechanical strain within bone and respond with mechanotransduction signals (e.g., calcium (Ca^{2+}), nitric oxide, extracellular ATP) and the expression of factors (e.g. receptor activator of NFκB ligand (RANKL) and sclerostin) that control the activity of bone resorbing osteoclasts and bone forming osteoblasts (Bonewald and Johnson, 2008; Klein-Nulend et al., 2013; Oftadeh et al., 2015; Rubin et al., 2006; Thompson et al., 2012; Turner et al., 2009). Given that fluid flow through the lacunar-canalicular network generates shear stress driving mechanotransduction in bone (Klein-Nulend et al., 2013), fluid flow is most often used to interrogate osteocyte response to mechanical load.

A number of commercially available (de Castro et al., 2015; Espinha et al., 2014; Genetos et al., 2005; Michael Delaine-Smith et al., 2015) and do-it-yourself (Aryaei and Jayasuriya, 2015; Burra et al., 2010; Shemesh et al., 2015) systems have been developed to model fluid flow in osteoblast and osteocyte-like cultured cells and each has its own limitations, such as limited throughput and/or functionality. We have designed a multifunctional fluid flow device (FFD) that when paired with standard 96 well culture plates and a commonly used fluid flow apparatus (e.g., peristaltic pump, syringe pump, pressurized or gravity flow system), provides the user a versatile, cost-effective device that can be easily used for both live cell imaging and molecular biology applications. Further, this device is scalable and can be adapted to medium-to-high throughput application.

2. Materials and methods

2.1. Cell Culture

UMR-106 rat osteoblast-like cells (ATCC) were cultured in DMEM media containing 10% FBS and cultured at 37°C, 5% CO_2, as described (Gupta et al., 2016). Media was changed every two to three days.

2.2 Device Design

The multi-functional FFD is designed for applying fluid flow to a single well of a typical 96 well assay plate (Fig. 1A). The FFD has an inlet port situated in the center of the well and an outlet port slightly offset to one side (Fig. 1B). The FFD is tapered to allow a firm fit in a single well of the multi-well plate (Fig. 1C). The FFD is designed to pair with any standard size 96 well assay plate and can be connected to any commercially available fluid flow control system (i.e., peristaltic pump, syringe pump, pressurized or gravity flow system). Furthermore, this device can be scaled up to accommodate larger tissue culture dishes and

can be multiplexed to apply fluid flow to multiple wells simultaneously within the 96 well plate.

2.2. Fluid Flow Simulation

SolidWorks 2015 Flow Simulation software was used to perform computation fluid dynamics on the FFD and simulate the flow environment inside the well during flow. The FFD was drawn to scale with a fully enclosed geometry. Two boundary conditions were set for the flow simulation, inlet pressure and outlet flow volume. The inlet pressure set to 542.85 dynes/cm^2 (calculated from our flow rate, 35 mL/min and tubing diameter, 1.5 mm) and set to pulsate at 6 Hz to simulate pulsatile flow from our peristaltic pump.

In order to determine the pressure, we used the known inlet diameter and flow rate. The flow velocity (cm/sec) was calculated using the known flow rate set by our pump and area of the inlet (calculated from the known diameter) using the equation:

$$v=\frac{Q}{A}$$

Where v = velocity, Q = flow rate, and A = area of the inlet. Using the calculated velocity, we determined the pressure in Pascals using the Navier-Stokes equation simplified to Bernoulli's equation:

$$\frac{1}{2}\rho V^2+p+\rho g z$$

where ρ = density, V = velocity, p = pressure, g = gravity, and z = height. In order for Bernoulli's principle to hold true for our system, the following assumptions were made: (1) flow buffer is a Newtonian fluid, (2) the flow is incompressible, and (3) there is no friction inside the flow. The outlet flow volume was set to 5.8×10^{-7} m^3/s. For all simulations, the flow buffer was assumed to be similar to water (i.e., density = 1 g/cm^3).

2.3. Calcium imaging

UMR106 cells (40,000 cells/cm^2) were seeded in an Ibidi μ-slide I and into a Corning 96 well special optics plate, which has an optically clear bottom for optimal fluorescence imaging. Cells were loaded with 5μM Fluo-4 AM ester for 30 minutes, washed, and allowed to rest for 15 minutes to allow dye de-esterification, as described (Kerr et al., 2015). Individual wells/slides were imaged on an inverted fluorescence microscope equipped with a mercury light source, Ludel excitation filter wheel (ex: 485) and a Photometrics Cool Snap HQ (em: 510-535). All imaging automation was controlled by IP Lab with methods previously described (Kerr et al., 2015). fluid flow was induced during real-time Ca^{2+}-imaging using the same Gilson Minipuls 3 peristaltic pump and the same 1.5 mm silicone tubing for both conditions. The pump flow rate was adjusted to achieve the same fluid flow stress in both vessels as previously reported for the Ibidi chambers(Huesa et al., 2010) and based on our computational fluid simulation for the FFD.

2.3. Western blotting

Western blots were performed on whole cell extracts from UMR106 cells prepared immediately following exposure to fluid flow, as described (Hebert and Stains, 2013). Blots were probed for phospho- or total ERK1/2 (Cell Signaling Technologies), phospho- or total-pan-PKC (Cell Signaling Technologies), and GAPDH (Millipore), as described (Niger et al., 2012; Niger et al., 2010). Western blots were quantitated using ImageJ, as described (Liu et al., 2015).

2.4. Statistical Analysis

Unless indicated, all data were an average of three independent experiments. Data are presented as mean ± standard deviations. Data were assessed for statistical significance by student's t-test using GraphPad Prism (v6) (GraphPad Software, La Jolla, CA, USA). $P<0.05$ are considered statistically significant.

3. Results

3.1. Computational Fluid Dynamics

The results of the fluid flow simulation indicate that the fluid flows through the inlet of the FFD, where it impacts the bottom of the well and then spreads radially and evenly (Fig. 2A). Then the fluid flows up the walls of the well before being pulled through the outlet of the FFD, without interrupting the flow across the bottom of the well (Fig. 2B). In addition to flow trajectories, the computational solver calculated dynamic pressure (Fig. 3A), flow velocity (Fig. 3B), turbulence intensity (Fig. 3C) inside the well, and the average shear stress at the bottom surface of the well (Fig. 3D). Under the described conditions, the cell monolayer cultured on the bottom of the tissue culture vessel are subjected to a uniform average 4 dynes/cm^2 of shear stress (Fig. 3D). Further, the velocity trajectories indicate that the flow across the bottom surface of the well is uniform such that the entire well of cells will be subjected to the same forces (Fig. 2). The turbulence intensity within the system without the addition of cells is extremely low, 0.65% (Fig. 3C). These findings show that the FFD mimics physiologic fluid flow reported to be experienced by bone cells *in vivo* (Cardoso et al., 2013).

3.2. Device Validation

It is well established that osteoblasts, including UMR106 osteoblast-like cells, are mechano-responsive with fluid flow inducing a rapid influx of Ca^{2+} across the plasma membrane (Ban et al., 2011; Hung et al., 1995; Ishihara et al., 2013; Jing et al., 2013; Su et al., 2011; Suzuki et al., 2013; Thompson et al., 2012; Xing et al., 2011; You et al., 2001; Zhang et al., 2006). We validated the FFD by comparing fluid flow-induced Ca^{2+} influx with this device to that obtained with the widely used Ibidi chamber; a commercially available device that allows biologically relevant laminar flow derived shear stress on cells cultured within the chambers. Comparing the response of UMR106 cells between both devices yielded virtually indistinguishable peak Ca^{2+} magnitudes and elevation/decay kinetics of Ca^{2+}-dependent fluorescence (Fig. 4). To validate that this Ca^{2+} influx is biologically relevant, western blot analysis was performed for activation of PKC signaling, a ubiquitous Ca^{2+}-dependent

signaling pathway. Indeed, a rapid phosphorylation of PKC was observed in response to FSS (Fig. 5.)

In addition to Ca^{2+} influx, fluid flow initiates ERK signaling in osteoblasts, including UMR106 cells (Kapur et al., 2004; Triplett et al., 2007; Wadhwa et al., 2002; Weyts et al., 2002). We tested the response of UMR106 cells seeded in a 96 well tissue culture plate and subjected the cells to 4 dynes/cm^2 of shear stress for 1 minute. After flow, the cells were immediately lysed and examined by western blot. Consistent with the literature, fluid flow-induced rapid activation of ERK signaling as indicated by an increase in phosphorylated-ERK (Fig. 5). These data support the notion that the FFD generates a physiologic conditions and biological responses comparable to the accepted commercially available methods.

3.3 Device Multiplexing

In order to demonstrate the multiplexing capability of the FFD to be used for simultaneous independent replicates, we performed western blot analysis on whole cell extracts from UMR106 cells subjected to fluid flow simultaneously in separate wells (Fig. 6A). Indeed, we observe similar activation of both phospho-ERK and phospho-PKC signaling across each well (Fig. 6B). These data demonstrate the consistent stimulation and biological responses among cells simultaneously exposed to fluid flow conditions across independent wells.

4. Discussion

We have designed a fluid flow device to enable cell-based assays of fluid flow-dependent mechanotransduction. This FFD addressed the lack of a cost-effective and functionally flexible platform for these measures. Our approach was to design a low-cost flexible perfusion apparatus that, when coupled with commercially available 96 well plates and commonly available perfusion apparatus, yields such a system. Importantly, model simulations revealed that the FFD delivers physiologically relevant fluid flow to cultured cells. We also show that fluid flow with the FFD yielded quantitatively similar results to those reported with a commercially available system (Huang et al., 2015; Hung et al., 1995; Roy et al., 2014). As in the Ibidi system, a uniform induction of Ca^{2+} influx is observed in all cells in response to fluid flow in the FFD regardless of the cell's position in the well, supporting the modeling of uniform fluid flow. Together the results support the FFD as a reliable and valid solution to the shortcomings of commercially available fluid flow systems (i.e., cost and functionality).

The design of the FFD yields several important advantages over other fluid flow systems. First, the FFD couples to commercially available 96 well plates. This format supports both imaging as well as molecular and biochemical analyses using the same device. Indeed, we were unable to recover sufficient amounts of protein from the Ibidi chambers to perform analysis of signaling events by western blotting, underscoring the multifunctional applicability of our device. Using the same device for every experiment, rather than a device specifically for imaging and another device specifically for molecular and biochemical analyses, reduces experimental variables (Anderson et al., 2006). Furthermore, this format also allows expandability to a medium-to-high throughput cell culture platform if multiple FFDs are used in the same plate with a multichannel peristaltic pump, obtaining fully

independent replicates for each sample. Supporting this notion, our western blotting data demonstrate the consistent biological response to fluid flow among simultaneously stimulated wells using the multiplex format. Second, the FFD supports various fluid flow systems, which expands the flexibility and versatility of this system. Taken together, the FFD design provides a flexibility in function that is unparalleled by any currently available commercial solutions. Third, a significant advantage of the FFD is the cost savings. Current commercial devices that incorporate a culture platform enclosed in a perfusion chamber can be prohibitively expensive. While these chambers are more cost effective than full commercial systems that cost upwards of $30K, the FFD presented here offers a significant cost-savings given the estimated cost of a few dollars per unit plus the cost of a 96 well plate.

In conclusion, the FFD presented here overcomes a variety of drawbacks that are associated with currently available models (Sorkin et al., 2004). This FFD is highly versatile in its functionality and cost substantially less. Also, the device delivers physiologically relevant fluid flow conditions to cells in monolayer culture. The device elicits biological responses in osteoblast-like cells similar to what is reported in the field (Huang et al., 2015; Hung et al., 1995; Roy et al., 2014). Overall, this device provides an improved method for studying the response of not only bone cells, but also any mechano-responsive cell type *in vitro* and will help advance the study of mechanotransduction.

Acknowledgement

This work was funded by a grant from NIH/NIAMS (AR036361) to JPS, (AR062554) to CWW and (AR059179) to RML and institutional training grants to JSL (NIGMS, T32 GM008181) and SRI (NIAMS, T32 AR007592).

Literature Cited

Anderson EJ, Falls TD, Sorkin AM, Knothe Tate ML. The imperative for controlled mechanical stresses in unraveling cellular mechanisms of mechanotransduction. Biomedical engineering online. 2006; 5:27. [PubMed: 16672051]

Aryaei A, Jayasuriya AC. The effect of oscillatory mechanical stimulation on osteoblast attachment and proliferation. Materials science & engineering. C, Materials for biological applications. 2015; 52:129–134. [PubMed: 25953549]

Ban Y, Wu YY, Yu T, Geng N, Wang YY, Liu XG, Gong P. Response of osteoblasts to low fluid shear stress is time dependent. Tissue & cell. 2011; 43:311–317. [PubMed: 21764096]

Bonewald LF, Johnson ML. Osteocytes, mechanosensing and Wnt signaling. Bone. 2008; 42:606–615. [PubMed: 18280232]

Burra S, Nicolella DP, Francis WL, Freitas CJ, Mueschke NJ, Poole K, Jiang JX. Dendritic processes of osteocytes are mechanotransducers that induce the opening of hemichannels. Proceedings of the National Academy of Sciences of the United States of America. 2010; 107:13648–13653. [PubMed: 20643964]

Cardoso L, Fritton SP, Gailani G, Benalla M, Cowin SC. Advances in assessment of bone porosity, permeability and interstitial fluid flow. Journal of biomechanics. 2013; 46:253–265. [PubMed: 23174418]

de Castro LF, Maycas M, Bravo B, Esbrit P, Gortazar A. VEGF Receptor 2 (VEGFR2) Activation Is Essential for Osteocyte Survival Induced by Mechanotransduction. Journal of cellular physiology. 2015; 230:278–285. [PubMed: 25102966]

Espinha LC, Hoey DA, Fernandes PR, Rodrigues HC, Jacobs CR. Oscillatory fluid flow influences primary cilia and microtubule mechanics. Cytoskeleton. 2014; 71:435–445. [PubMed: 25044764]

Genetos DC, Geist DJ, Liu D, Donahue HJ, Duncan RL. Fluid shear-induced ATP secretion mediates prostaglandin release in MC3T3-E1 osteoblasts. Journal of bone and mineral research : the official journal of the American Society for Bone and Mineral Research. 2005; 20:41–49.

Gupta A, Anderson H, Buo AM, Moorer MC, Ren M, Stains JP. Communication of cAMP by connexin43 gap junctions regulates osteoblast signaling and gene expression. Cellular signalling. 2016; 28:1048–1057. [PubMed: 27156839]

Hebert C, Stains JP. An intact connexin43 is required to enhance signaling and gene expression in osteoblast-like cells. Journal of cellular biochemistry. 2013; 114:2542–2550. [PubMed: 23744706]

Huang LW, Ren L, Yang PF, Shang P. Response of Osteoblasts to the Stimulus of Fluid Flow. Critical reviews in eukaryotic gene expression. 2015; 25:153–162. [PubMed: 26080609]

Huesa C, Helfrich MH, Aspden RM. Parallel-plate fluid flow systems for bone cell stimulation. Journal of biomechanics. 2010; 43:1182–1189. [PubMed: 20031135]

Hung CT, Pollack SR, Reilly TM, Brighton CT. Real-time calcium response of cultured bone cells to fluid flow. Clinical orthopaedics and related research. 1995:256–269. [PubMed: 7641488]

Ishihara Y, Sugawara Y, Kamioka H, Kawanabe N, Hayano S, Balam TA, Naruse K, Yamashiro T. Ex vivo real-time observation of Ca(2+) signaling in living bone in response to shear stress applied on the bone surface. Bone. 2013; 53:204–215. [PubMed: 23246671]

Jaalouk DE, Lammerding J. Mechanotransduction gone awry. Nature reviews. Molecular cell biology. 2009; 10:63–73. [PubMed: 19197333]

Jing D, Lu XL, Luo E, Sajda P, Leong PL, Guo XE. Spatiotemporal properties of intracellular calcium signaling in osteocytic and osteoblastic cell networks under fluid flow. Bone. 2013; 53:531–540. [PubMed: 23328496]

Kapur S, Chen ST, Baylink DJ, Lau KH. Extracellular signal-regulated kinase-1 and -2 are both essential for the shear stress-induced human osteoblast proliferation. Bone. 2004; 35:525–534. [PubMed: 15268905]

Kerr JP, Robison P, Shi G, Bogush AI, Kempema AM, Hexum JK, Becerra N, Harki DA, Martin SS, Raiteri R, Prosser BL, Ward CW. Detyrosinated microtubules modulate mechanotransduction in heart and skeletal muscle. Nature communications. 2015; 6:8526.

Klein-Nulend J, Bakker AD, Bacabac RG, Vatsa A, Weinbaum S. Mechanosensation and transduction in osteocytes. Bone. 2013; 54:182–190. [PubMed: 23085083]

Liu S, Niger C, Koh EY, Stains JP. Connexin43 Mediated Delivery of ADAMTS5 Targeting siRNAs from Mesenchymal Stem Cells to Synovial Fibroblasts. PloS one. 2015; 10:e0129999. [PubMed: 26076025]

Michael Delaine-Smith R, Javaheri B, Helen Edwards J, Vazquez M, Rumney RM. Preclinical models for in vitro mechanical loading of bone-derived cells. BoneKEy reports. 2015; 4:728. [PubMed: 26331007]

Niger C, Buo AM, Hebert C, Duggan BT, Williams MS, Stains JP. ERK acts in parallel to PKCdelta to mediate the connexin43-dependent potentiation of Runx2 activity by FGF2 in MC3T3 osteoblasts. American journal of physiology. Cell physiology. 2012; 302:C1035–1044. [PubMed: 22277757]

Niger C, Hebert C, Stains JP. Interaction of connexin43 and protein kinase C-delta during FGF2 signaling. BMC biochemistry. 2010; 11:14. [PubMed: 20338032]

Oftadeh R, Perez-Viloria M, Villa-Camacho JC, Vaziri A, Nazarian A. Biomechanics and mechanobiology of trabecular bone: a review. Journal of biomechanical engineering. 2015; 137

Roy B, Das T, Mishra D, Maiti TK, Chakraborty S. Oscillatory shear stress induced calcium flickers in osteoblast cells. Integrative biology : quantitative biosciences from nano to macro. 2014; 6:289–299. [PubMed: 24445362]

Rubin J, Rubin C, Jacobs CR. Molecular pathways mediating mechanical signaling in bone. Gene. 2006; 367:1–16. [PubMed: 16361069]

Shemesh J, Jalilian I, Shi A, Heng Yeoh G, Knothe Tate ML, Ebrahimi Warkiani M. Flow-induced stress on adherent cells in microfluidic devices. Lab on a chip. 2015; 15:4114–4127. [PubMed: 26334370]

Sorkin AM, Dee KC, Knothe Tate ML. “Culture shock” from the bone cell's perspective: emulating physiological conditions for mechanobiological investigations. American journal of physiology. Cell physiology. 2004; 287:C1527–1536. [PubMed: 15317661]

Su JH, Xu F, Lu XL, Lu TJ. Fluid flow induced calcium response in osteoblasts: mathematical modeling. Journal of biomechanics. 2011; 44:2040–2046. [PubMed: 21665208]

Suzuki T, Notomi T, Miyajima D, Mizoguchi F, Hayata T, Nakamoto T, Hanyu R, Kamolratanakul P, Mizuno A, Suzuki M, Ezura Y, Izumi Y, Noda M. Osteoblastic differentiation enhances expression of TRPV4 that is required for calcium oscillation induced by mechanical force. Bone. 2013; 54:172–178. [PubMed: 23314072]

Thompson WR, Rubin CT, Rubin J. Mechanical regulation of signaling pathways in bone. Gene. 2012; 503:179–193. [PubMed: 22575727]

Triplett JW, O'Riley R, Tekulve K, Norvell SM, Pavalko FM. Mechanical loading by fluid shear stress enhances IGF-1 receptor signaling in osteoblasts in a PKCzeta-dependent manner. Molecular & cellular biomechanics : MCB. 2007; 4:13–25. [PubMed: 17879768]

Turner CH, Warden SJ, Bellido T, Plotkin LI, Kumar N, Jasiuk I, Danzig J, Robling AG. Mechanobiology of the skeleton. Science signaling. 2009; 2:pt3. [PubMed: 19401590]

Wadhwa S, Godwin SL, Peterson DR, Epstein MA, Raisz LG, Pilbeam CC. Fluid flow induction of cyclo-oxygenase 2 gene expression in osteoblasts is dependent on an extracellular signal-regulated kinase signaling pathway. Journal of bone and mineral research : the official journal of the American Society for Bone and Mineral Research. 2002; 17:266–274.

Weyts FA, Li YS, van Leeuwen J, Weinans H, Chien S. ERK activation and alpha v beta 3 integrin signaling through Shc recruitment in response to mechanical stimulation in human osteoblasts. Journal of cellular biochemistry. 2002; 87:85–92. [PubMed: 12210725]

Xing Y, Gu Y, Xu LC, Siedlecki CA, Donahue HJ, You J. Effects of membrane cholesterol depletion and GPI-anchored protein reduction on osteoblastic mechanotransduction. Journal of cellular physiology. 2011; 226:2350–2359. [PubMed: 21660958]

You J, Reilly GC, Zhen X, Yellowley CE, Chen Q, Donahue HJ, Jacobs CR. Osteopontin gene regulation by oscillatory fluid flow via intracellular calcium mobilization and activation of mitogen-activated protein kinase in MC3T3-E1 osteoblasts. The Journal of biological chemistry. 2001; 276:13365–13371. [PubMed: 11278573]

Zhang J, Ryder KD, Bethel JA, Ramirez R, Duncan RL. PTH-induced actin depolymerization increases mechanosensitive channel activity to enhance mechanically stimulated Ca2+ signaling in osteoblasts. Journal of bone and mineral research : the official journal of the American Society for Bone and Mineral Research. 2006; 21:1729–1737.

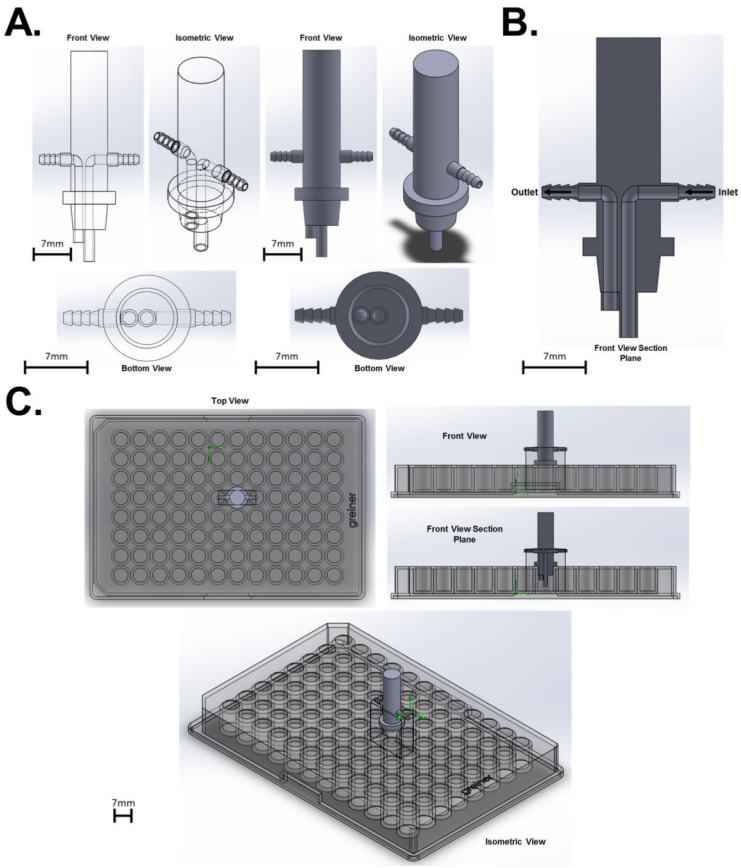

Figure 1.

Computer rendering of the novel FFD. (A) Design of the FFD. (B) Section cut of the FFD to show the inlet and outlet channels within the device. (C) The FFD interfacing with a typical 96 well assay plate.

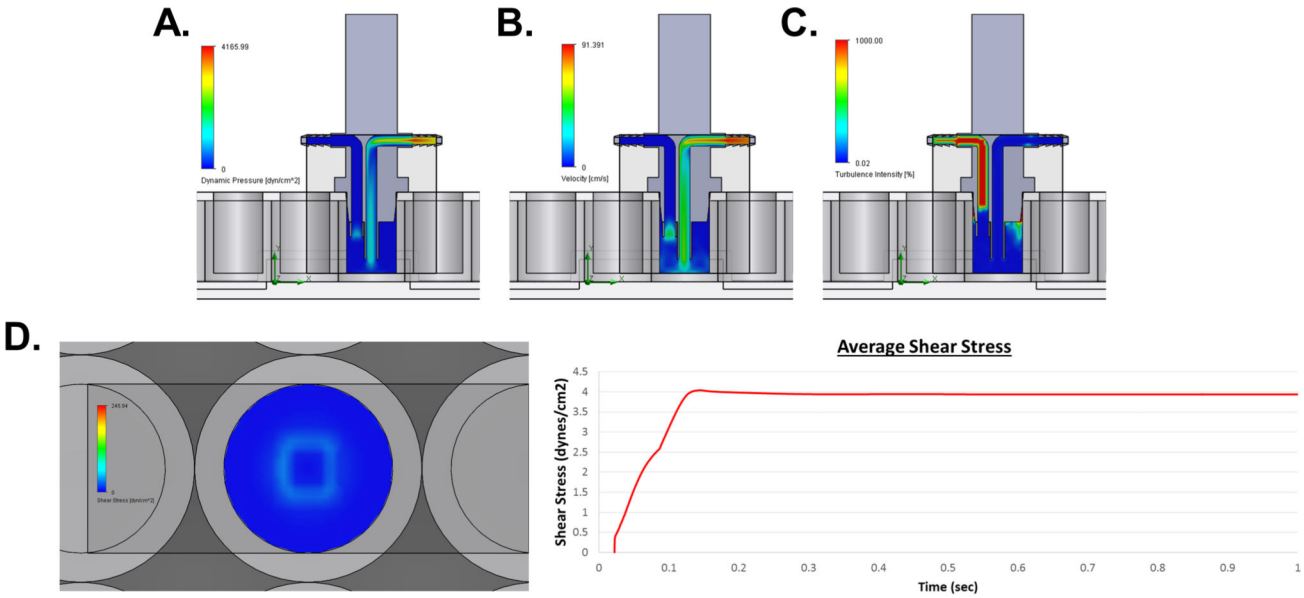

Figure 2.

Vector lines indicating fluid flow trajectories. (A) Trajectories of flow from the front section view and a top view. (B) Up close view of the inlet and outlet trajectories within the well of the plate. Data were determined using SolidWorks 2015 Flow Simulation software.

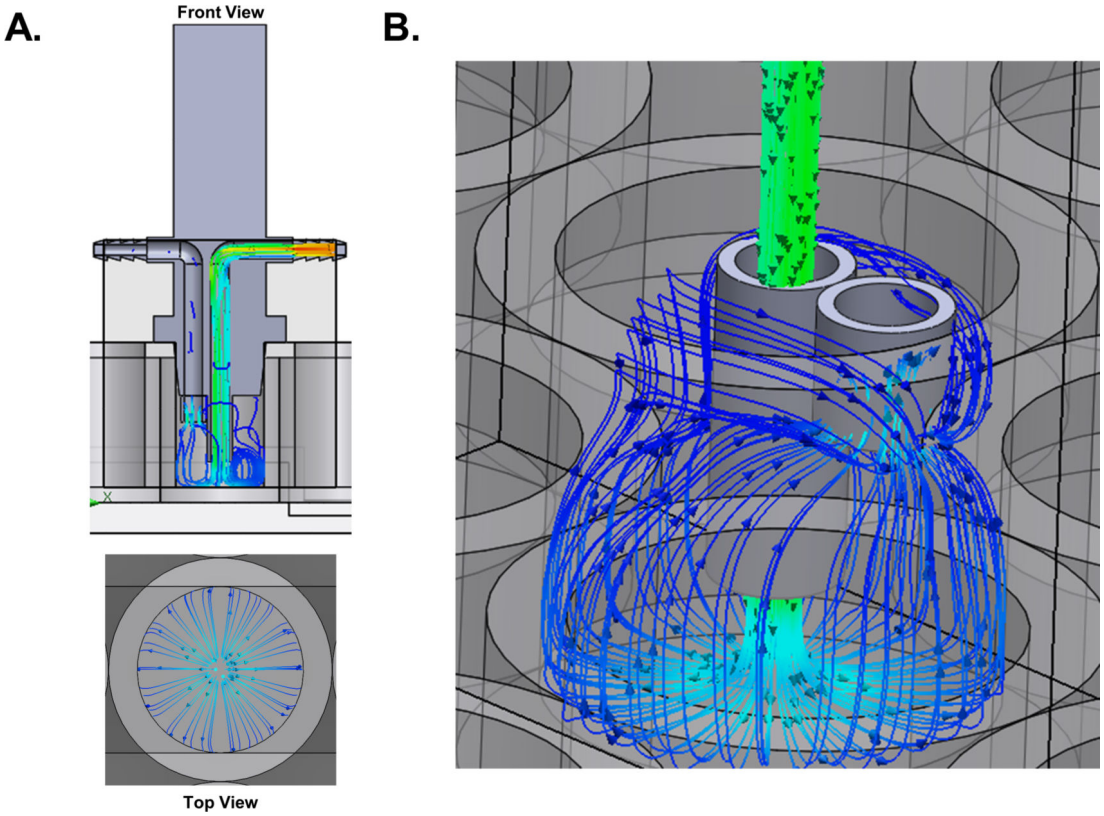

Figure 3.

Computational fluid dynamics. (A) Simulated dynamic pressure within the device and well. (B) Simulated velocity within the device and well. (C) Simulated turbulence intensity within the device and well. (D) Simulated shear stress at the bottom surface of the well. Computational trace of the average shear stress at the bottom surface of the well over time. Data were determined using SolidWorks 2015 Flow Simulation software.

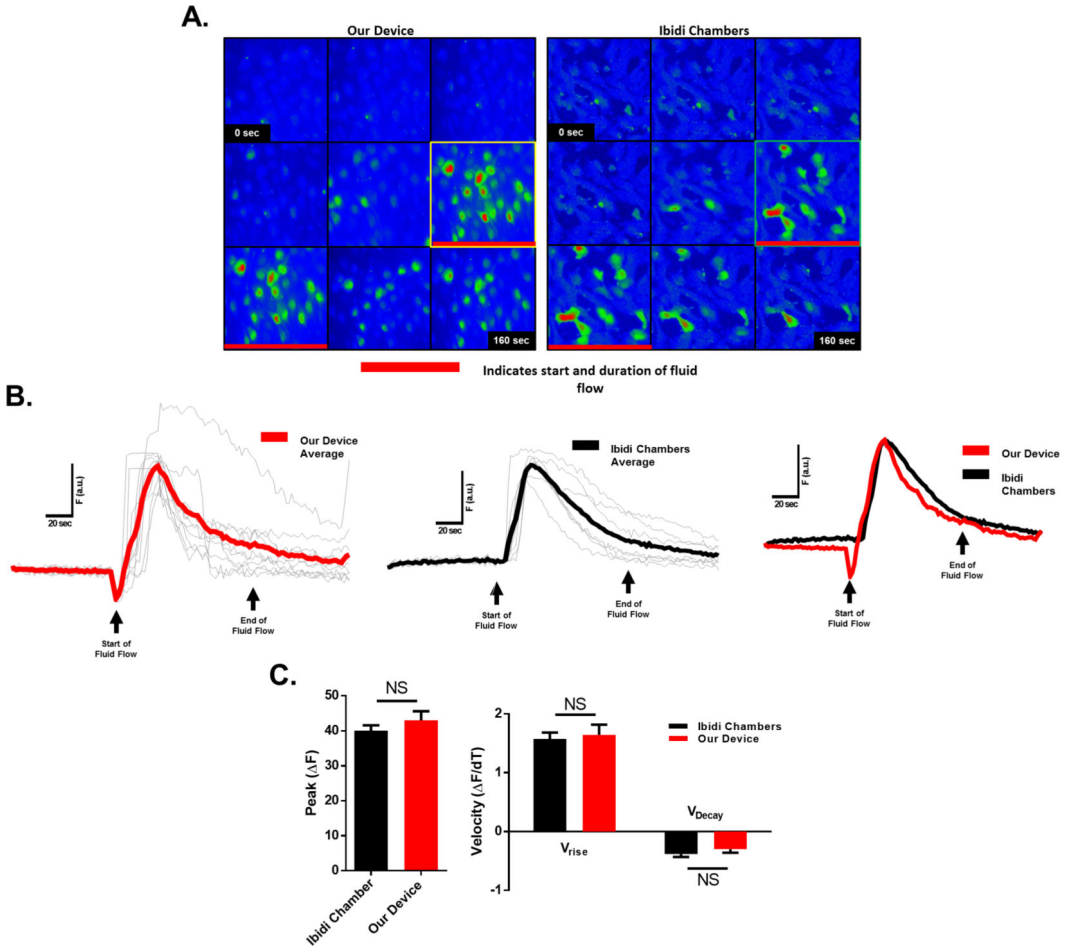

Figure 4.

Real-time Ca^{2+} imaging of UMR106 cells during application of fluid flow. (A) Fluo-4 Ca^{2+} indicator dye fluorescence before (basal) and during flow (response) of cells seeded in both the Ibidi chambers and a 96 well plate with the FFD. Red line in image sequence indicates start and duration of fluid flow. Highlighted boxes indicate peak calcium responses. (B) Traces of average Ca^{2+} indicator dye fluorescence intensity over time scaled to same basal level of fluorescence intensity are shown in bold lines. Gray overlay traces represent the Ca^{2+} response of individual cells in the well. (C) Peak change in Ca^{2+} indicator dye fluorescence intensity and elevation/decay kinetics of Ca^{2+}-dependent fluorescence. NS, not statistically significant.

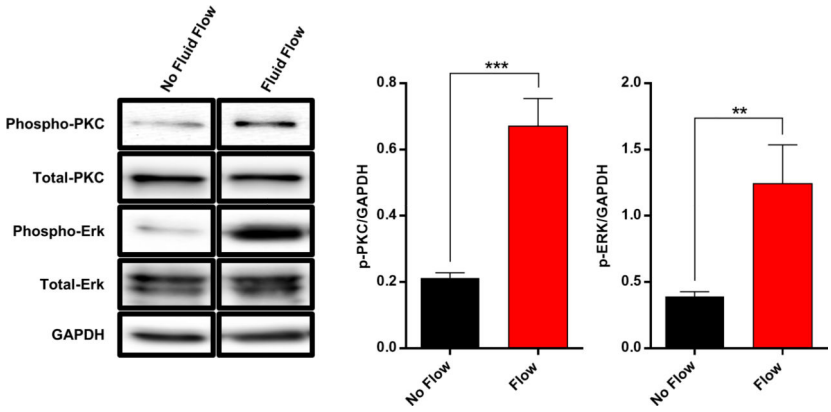

Figure 5.

Western blot analysis of UMR106 cells exposed to fluid flow in the FFD. Fluid flow induced rapid activation of PKC signaling and ERK signaling as indicated by an increase in phosphorylated PKC and phosphorylated ERK. Data are from the same gel and exposure. ImageJ quantification of western blot relative to GAPDH. Double asterisks (**) indicate statistical significance at $p<0.01$. Triple asterisks (***) indicate statistical significance at $p<0.001$.

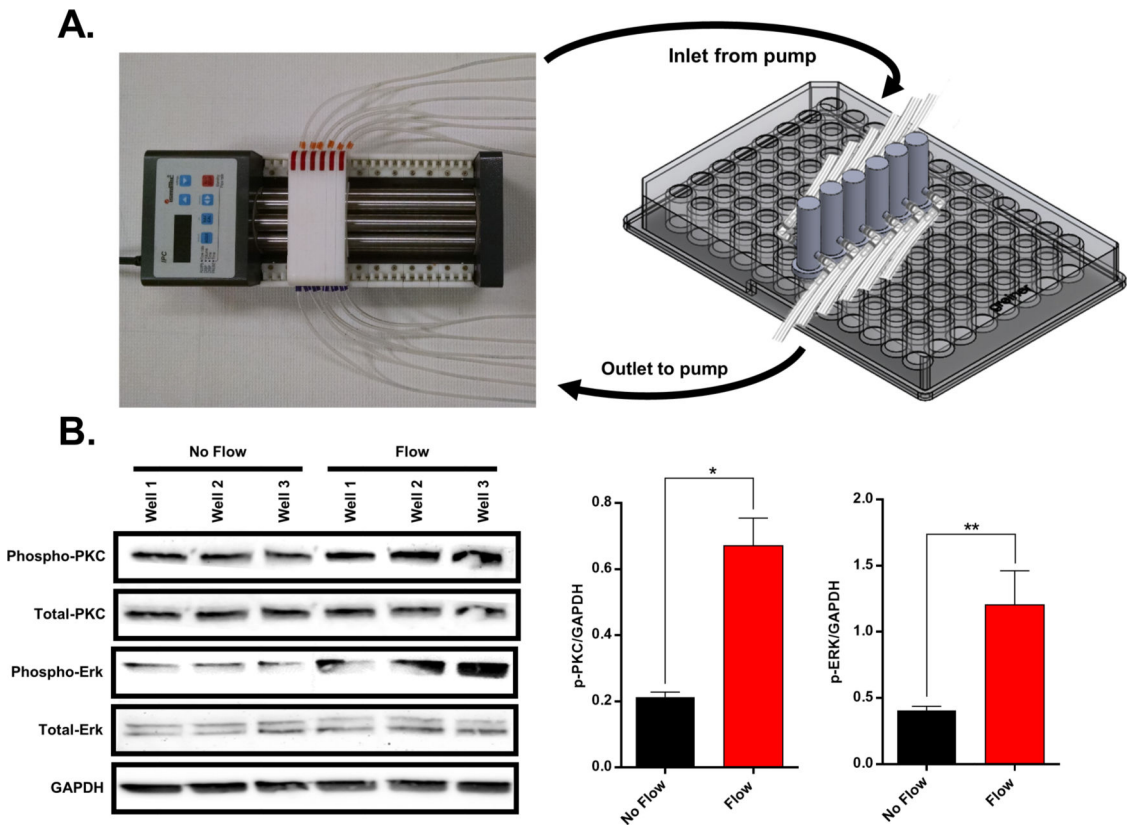

Figure 6.

Demonstration of the multiplexing capability of the FFD. (A) Example of the multi-channel peristaltic pumped used when multiplexing the FFD and a computer rendering of the FFD multiplexed in a single 96 well assay plate across 6 independent wells. (B) Western blot analysis of UMR106 cells simultaneously exposed to fluid flow in separate wells. ImageJ quantification of western blot analysis relative to GAPDH. Asterisks indicate statistical significance at $p<0.05$. Double asterisks (**) indicate statistical significance at $p<0.01$.